Purification, structural characterization, and cognitive improvement activity of a polysaccharides from Schisandra chinensis

Mengjie Xu, Tingxu Yan, Guowei Gong, Bo Wu, Bosai He, Yiyang Du, Feng Xiao, Ying Jia

PII: S0141-8130(20)33730-2

DOI: https://doi.org/10.1016/j.ijbiomac.2020.06.275

Reference: BIOMAC 16032

To appear in: *International Journal of Biological Macromolecules*

Received date: 2 March 2020

Revised date: 27 June 2020

Accepted date: 29 June 2020

Please cite this article as: M. Xu, T. Yan, G. Gong, et al., Purification, structural characterization, and cognitive improvement activity of a polysaccharides from Schisandra chinensis, *International Journal of Biological Macromolecules* (2020), https://doi.org/10.1016/j.ijbiomac.2020.06.275

Purification, structural characterization, and cognitive improvement activity of a polysaccharides from Schisandra chinensis

MengjieXu[a#], Tingxu Yan[b#], Guowei Gong[c], Bo Wu[b], Bosai He[b], Yiyang Du[b], Feng Xiao[b*], Ying Jia[b*]

[a] School of Traditional Chinese Materia Medica, Shenyang Pharmaceutical University, Wenhua Road 103, Shenyang 110016, China

[b] School of Functional Food and Wine, Shenyang Pharmaceutical University, Wenhua Road 103, Shenyang 110016, China

[c] Department of Bioengineering, Zunyi Medical University, Zhuhai Campus, Zhuhai, Guangdong, 519041, China

[#] Mengjie Xu and Tingxu Yan contributed equally to this work

[*] Corresponding authors:

Ying Jia, School of Functional Food and Wine, Shenyang Pharmaceutical University, Wenhua Road 103, Shenyang, 110016, PR China. E-mail address: jiayingsyphu@126.com.

Feng Xiao, School of Functional Food and Wine, Shenyang Pharmaceutical University, Wenhua Road 103, Shenyang, 110016, PR China. E-mail address: 48461290@qq.com

Abstract

The present study aimed to evaluate structural characteristics of a polysaccharides, SCP2-1, isolated from *Schisandra chinensis* (Turcz.) Baill (*S. chinensis*) and to assess its improvement on cognitive dysfunction caused by excessive neuroinflammation. Structural characterization indicated that SCP2-1 was composed of glucose and galactose in a molar ratio of 8.78: 1.23 with molecular weight of 5.388 KDa. The main linkages of the glycosidic bonds of SCP2-1were 1,4-linked-Glcp, 1,4-linked-Galp, 1-linked-Galp and 1,4,6-linked-Galp. The evaluation of behavioral pharmacology and the detection of biochemical markers exhibited that SCP2-1 could improve LPS-induced cognitive dysfunction in mice, ameliorate excessive inflammatory response. The results showed that SCP2-1 could ameliorated the animals' exploration time of novel arm in Y maze test, shortened the escape latency of mice in MWM test, and increased the exploration time of new object in NOR test. What' more, mice could improve histopathological changes induced by LPS, suppress the over-activation of glial cells, decrease the expression of proinflammatory cytokines, increase the levels of anti-inflammatory cytokines, reduce the levels of NLRP3, M-caspaes-1, which may further induce the decrease of excessive deposition of Aβ. Furthermore, SCP2-1 could inhibit the over-activation of NF-κB and the hyperphosphorylation of P38 MAPK pathway.

Key words: Schisandra chinensis polysaccharides, Structural characterization, Neuroprotection

1. Introduction

Inflammation is a kind of defense reaction produced by the body under harmful stimulation. However, during the process of chronic inflammatory disease, pro-resolving activities are not neutralize the proinflammatory signaling entirely, for neuroinflammation, such as exogenous injury, excessive Aβ deposition, and long-term peripheral inflammation, these inflammation is further aggravated through cellular debris, dead cell and the change in microenvironment of damaged tissue, leading to disease, include Alzheimer's disease (AD), one of the most common type of neurodegenerative dementia. Emerging studies suggest that neuroinflammation is not an ensuing system activated by accumulated Aβ, but instead, contributes as much or more to pathogenesis as plaques themselves [1, 2]. Glial cells play a considerable role in CNS immunity. Once activated, glial cells produce fertility promoting cytokines, such as TNF-α, NO, COX2, IL-6 and IL-1β, through MAPKs family and NF-κB pathway. Microglia, in particular, possessed the function of tracking andphagocytosis of Aβ, which is very important for the brain to maintain the balance of Aβ[3, 4]. Although the research on the pathogenesis of AD has never stopped, no effective treatment to prevent and ameliorate this disease has been found. The researchers began to turn their attention to immunomodulatory therapy[5].

Polysaccharide are macromolecules composed of monosaccharide units linked by glycosidic bonds. As the increasing studies in immunomodulatory, the mechanism of polysaccharides starting to be linked with neuroinflammation[6, 7]. A large number of polysaccharides have been reported to have positive effects on modulating over-active inflammatory response, and some of them could improve cognitive function by regulating the immune response[8]. *S. chinensi*s is a well-known and widely used traditional Chinese herbal medicine. Studies have showed that the crude polysaccharide from *S. chinensis* have multiple effects including antioxidant, antiaging, anti-diabetic activities, etc[9-11]. Our previous studies have shown that SCP could improve cognitive impairment in mice[12]. In this study, we isolated a water-soluble polysaccharide from *S. chinensis*, SCP2-1. Structural characterization

was investigated to elucidated the preliminary structure of SCP2-1, and meanwhile provide insight investigation of its effects on over-activated inflammation in mice with AD, which might be related to its structural feature, paving the way for its further utilization.

2. Materials and methods

2.1. Materials

The *S. chinensis* was purchased from TONGRENTANG Co., Ltd. (Shenyang, Liaoning Province, China). LPS (PubChem CID: 11970143) were obtained from Sigma–Aldrich (St. Louis, MO, USA). All other chemical reagents and solvents were purchased from Beyotime Biotechnology Co. Ltd. (Jiangsu, China). All primary antibodies were purchased from Abcam (Cambridge, MA, USA).

2.2 Preparation of polysaccharides

S. chinensis were dried at 60℃ for 24 h. The powder of *S. chinensis* was defatted with petroleum ether (boiling range: 30℃-60℃) three times at ultrasonic for 2h. After defatting, *S. chinensis* were extracted with the water (1:10, w/v) two times at 80℃ for 5 h. Combined and concentrated extracts, added alcohol under stirring, until the concentration of the alcohol reached 80% and kept overnight at 4℃. Re-dissolved the precipitate with water, subjected the solution to Sevage reagent to remove the proteins until no peak of UV scanning at 260 nm and 280nm. After dialysis, crude polysaccharides (SCP) were obtained via freeze-drying. SCP was applied to DEAE-Sephadex Fast Flow cellulose column (2.5×70 cm) equilibrated with distilled water. Fractionated and eluted the SCP of NaCl solutions with different concentrations (0, 0.05, 0.1, 0.15 mol/L) at 1.5 mL/min, respectively. Combined main fractions according to the total carbohydrate content quantified by the anthranone–sulfuric acid method. The second fraction, SCP2, was further fractionated with Sephadex CL-6B column (1.6×50 cm), and eluted with 0.15 M NaCl at 0.5 mL/min. Collected, concentrated, dialyzed (MWCO 3500 Da) and lyophilized the fraction to obtain a white purified polysaccharide (SCP2-1). SCP2-1 was sealed and placed in a cool place for future study.

2.3 Characterization structure of SCP2-1

2.3.1 Detection of molecular weight

Dissolved SCP2-1 (2 mg) in distilled water (1 mL) and applied it to a high-performance liquid chromatograph (Agilent 1260, USA) equipment with gel-filtration chromatographic column. The mobile phase was 50 mM NaCl solution with a flow rate of 0.8 mL/min. The injection volume was 20 μL and the molecular weight was determined by GPC software.

2.3.2. Analysis of Monosaccharide compositional

Hydrolyzed SCP2-1 (5 mg) in 0.2 M TFA for 30 min and evaporated to dryness. Removed residual TFA under reduced pressure. The residue reacted with pyridine (1 mL), hexamethyldisilazane (0.4 mL) and trimethylchlorosilane (0.2 mL) at 80℃ for 30 min, then 1 mL distilled water was added. The trimethylsilylated derivatives were analyzed by GC-MS (Shimadzu GCMS-QP 2010) with RXI-5 SIL MS capillary column (30 m × 0.25 μm × 0.25 μm). Analysis conditions as follow: Helium was used as the carrier gas with a flow rate of 1 mL/min. The column temperature raised to 280°C with a rate of 4°C/min and held for 5 min. The temperature of inlet and detector was 250°C and 280°C respectively.

2.3.3. Chemical derivative analysis.

The sample was dissolved in DMSO, then added 200 mg NaOH. 1.5 mL methyl iodide was added after stirring for 4 h. Placed the mixture in the dark for 2 h and add distilled water. The product was then extracted with 3 mL chloroform and dried under reduced pressure. The residues were hydrolyzed with 10 mL TFA (2 mol/L) for 8 h and then dissolved into 1% NaOH (4 mL). After reduction, added 10 mg $NaBH_4$ and 100 μL glacial acetic acid. The sample was dried under reduced pressure, acetylated with 1.5 mL acetic anhydride and pyridine for 2 h at 100°C. The acetylated derivatives were extracted with 4 mL chloroform. The analysis conditions were similar to 2.3.2 by GC-MS.

2.3.4. NMR analysis

Dissolved sample powder (10mg) in 0.5 mL D_2O and analyzed the solution by a high-resolution NMR spectrometer (AVANCE 600, Bruker, Germany). The NMR chemical shifts of One-dimensional (^1H and ^{13}C) and Two-dimensional (^1H-^1H COSY,

NOESY, HSQC, HMBC) were measured by NMR tested and presented in ppm.

2.3.5. FT-IR analysis

The sample (2mg) were ground with potassium bromide (200mg) and pressed into slice. Fourier transform infrared spectrum of the sample was detected by Fourier transform infrared spectrum spectrometer (GANGDONG SCI.&TECH. CO,.LTD, China) at the wavelength range of 400–4000 cm^{-1}.

2.4 Evaluation of the neuroprotection activities of SCP2-1

2.4.1 Animals and behavior test

KM mice (male) weighing 22±2 g were obtained from the Central Animal House of Shenyang Pharmaceutical University (Shenyang, China). After adaptation period, animals were divided into 4 groups randomly (n=10-12): control, model, donepezil (PubChem CID: 5741) and SCP2-1 group. The mice received daily treatment (i.g.) (56 mg/kg) for 3 weeks. On the last 9 days, mice except control was intraperitoneal injected with LPS (0.25 mg/kg) 2 h before drug administration.

Y-maze was used to measure short-term memory of mice. Placed the animals at the end of the "starting arm" and allowed them to explore (novel arm blocked off by a partition) for 15 min. After 3h, the partition was removed, the mice were allowed to return to the maze for exploration in 5 min. The times mice explored each arm was counted. Novel place/object recognition (NOR) test was carried out to measure pattern separation. Mice was introduced to explore two objects for 5 min, then. One novel object placed on the opposite end of the arena, and mice returned to the arena after 30 min. Exploratory behavior of mice during the 5-min testing period was recorded. Morris Water Maze (MWM) test was carried out to measure reference and retention memory. Briefly speaking, during the place navigation test, the mice were trained for five consecutive days to find and remember the position of the hidden platform. The animal was allowed to swim to the hidden platform. Regardless of whether mice find a platform within 60 s, mice were required to learn on the platform for 30 s. Escape latency was measured and recorded. After the place navigation test, the spatial memory of the animals was evaluated in the spatial probe test, the mice

were evaluated in a 60 s test without platform. The time mice spent in the target quadrant and the times mice crossed the platform position were recorded.

2.4.2 *Biochemical analysis*

2.4.2.1 ELISA Kit

The Elisa kits (MEIMIAN, Jiangsu, China) were used to measure TNF-α, IL-1β and IL-6 in mice according to the manufacture instructions.

2.4.2.2 RT-qPCR

Total RNA of samples was extracted from the hippocampal by RNAiso Plus. Synthesized the first strand cDNA with the reverse transcription kit, and assayed the relative mRNA expressions of the TNF-α, IL-1β and IL-6 gens by quantitative real time PCR kit. The PCR primer sequences were shown in Supplementary data. Used β-actin as control.

2.4.2.3 HE Staining

The brain tissues were embedded in paraffin and cut into slices, the specimens were stained with H.E. for observing the histological changes.

2.4.2.4 Immunohistochemistry

Preincubated slices with 10% normal goat serum containing 0.2% Triton × 100 at 37°C for 1 h. Slides were then incubated over night at 4°C with GFAP and Iba-1 primary antibodyin 2% serum. After washed in PBS, slides was incubated with secondary antibody for 1 h at 37°C. Then, sections were washed in PBS three times and covered with DAPI/Fluorescence quenching agent. The images were collected by fluorescence microscopy.

Sections of brain tissue were incubated with normal goat serum for 20 min, then incubated with Aβ antibody (1:1000) overnight at 4℃. After incubation, the sections were washed with PBS and incubated with secondary antibody for 45 min. They were incubated with streptavidin-biotin HRP complex. Samples were stained with DAB and hematoxylin.

2.4.2.5 Western Blot

RIPA Buffer was used to extract total protein from hippocampal tissues. The concentrations were detected by BCA kit. Separated the proteins by SDS-PAGE for 90 min, then transferred it to nitrocellulose filter membrane. Blocked the membranes with 5% skim milk which dissolved in at 37℃ for 2 h and probed with antibodies against cathepsin B, NLRP3, M-caspase-1, pro-caspase-1, IL-4, IL-10, ERK1/2, JNK, P38, p-ERK1/2, p-JNK, p-P38 and β-actin (1:1000 dilution), overnight at 4℃. The next day, membranes were incubated with the corresponding HRP-labeled secondary antibodies. Used ECL reagent, to make immunoreactive bands. Detected and analyzed signals by Image pro plus.

2.5. Statistical analysis

All data were presented as the mean ± SD with normal distribution. The significance of differences in data between the groups were determined by one-way or two-way ANOVA followed by Turkey's test for equality of variances using Graphpad Prism 7.0. Differences were considered statistically significant at $p < 0.05$.

3. Results

3.1. Characterization of SCP2-1

3.1.1. Preparation of SCP2-1

SCP was extracted by hot water with a yield of 7.93%. As shown in Fig. 1, two main fractions were obtained and designated as SCP1 and SCP2. SCP1 and SCP2 accounted for 28.3% and 32.1% of the total SCP content, respectively. SCP2 were further purified through Sephadex CL-6B column chromatography and eluted with 0.15 mol/L NaCl. A single, symmetrical peak (SCP2-1) were obtained and selected. The Mw of SCP2-1 was identified to be 5.388×10^3 Da by HPGPC and SCP2-1 was used for the further experiments (Fig. 1). The purity of the polysaccharide and protein content of SCP2-1 were detected by Phenol sulfuric acid method, Bradford assay, respectively. The results showed that the total sugar and protein contents of SCP2-1were 97.82%, 0.75%, respectively.

[Fig. 1]

3.1.2. Monosaccharide composition and Glycosidic linkage

The GC-MS spectra profile of the SCP2-1 presented two peaks with the retention time of 32.242 min and 32.901 min, which suggest SCP2-1 was composed of glucose and galactose with a molar ratio of 8.78: 1.23 (Fig. 2A). The glycosidic linkage of SCP2-1 was detected by methylation method and analyzed by GC-MS. As shown in Table 2, the 1-linked-Galp, 1,4-linked-Galp, 1,4-linked-Glcp and 1,4,6-linked-Galp were identified in SCP2-1 (Table 1).

[Table 1]

3.1.3 NMR spectrum characterization

1 D and 2 D NMR spectra of SCP2-1 were shown in Fig. 2B-G. No signal in low field, indicating that SCP2-1 did not contain aldehydes[13]. In ^{13}C and DEPT NMR spectra, four anomeric carbon signals were found at δ_C 105.84, 105.73, 102.82 and 100.95 ppm. In the ^{1}H-NMR spectrum, four kinds of anomeric proton signals were found at δ_H 5.32, 4.57, 4.56 and 4.40 ppm, the signal at δ_H 5.32 ppm was induced by H-1 of *α*-glucopyranosyl residue, which is consistent with FT-IR data (Supplementary Fig. 3)[14]. HSQC spectra showed the signal at δ_C 101.0 in ^{13}C NMR spectrum was assigned to C-1 of *α*-glucopyranosyl residue. ^{1}H-^{1}H COSY spectra incicated the shift of H-2, H-3 and H-4 of *α*-D-glucopyranosyl residue were δ_H 3.55, 3.89 and 3.57 ppm, respectively. Combined with NOSY, the shift of H-5 was 3.76 ppm. Other major Glcp signals were easily identified and assigned by ^{13}C-NMR and HSQC. Similarly, the assignments could be determined respectively, all the NMR signals of residues were assigned in Table 2.

The sequence of glycosidic linkage SCP2-1 was identify by HMBC spectrum. There was an obvious cross-peak ($\delta_{H,C}$ 5.32, 78.2 ppm) indicated existence of the sequence of [→4)-*α*-Glcp-(1→4)-*α*-Glcp-(1→]. The cross peaks of δ_C 105.7 ppm and δ_H 3.57 ppm indicated the presence of the sequence [→4)-*β*-Galp-(1→4)-*α*-Glcp-(1→]. The peak at *δ*5.32/78.2 indicated that residue 1, 4, 6-*β*-Galp was linked with 1,4-*α*- Glcp at C-4 position. The cross peaks of δ_C 105.8 ppm and δ_H 3.81 ppm showed 1-*β*-Galp residues branched at O-6 of 1,4,6-*β*-Galp. The structure of SCP2-1was proposed as shown in Fig. 2H.

The infrared spectrum of SCP2-1 was shown in Supplementary Fig. 3. The intense and broad brand at 3367 cm^{-1} was attributed to the stretching vibrations of O-H. The absorption band at 2925 cm^{-1} is derived from the C-H stretching vibration of -CH2-. The results of FTIR preliminarily indicate that SCP2-1 is a neutral polysaccharide.

[Fig. 2]

[Table 2]

[Supplementary Fig. 3]

3.2 Neuroprotective effect of SCP2-1

3.2.1 Cognitive ability of mice

The experiment schedule shown in Fig. 3A.

As shown in Fig. 3B-D, LPS significantly decreased novel arm entries compared with control group in Y maze test ($p<0.05$), indicating an impairment of working memory, which could be antagonized by donepezil and SCP2-1 treatment ($p<0.05$ and $p=0.073$, Compared with model group, respectively). There was no significant difference of the total number of arm entries among these groups.

In NOR test, the results suggested that LPS significantly reduced the exploration times of mice to novel objects ($p <0.01$ and $p>0.05$, compared the exploration time between old and novel objects of mice in the con and mod group, respectively), which indicated that the mice had impaired short-term memory, administration of donepezil and SCP2-1 normalized performance of mice ($p <0.05$ compared the exploration time between old and novel objects of mice in the Don and SCP2-1 group) (Fig. 3E-G).

During MWM test, mice injected with LPS took longer time to find the platform compared to the normal one ($p<0.05$, on the second and fourth days; $p<0.01$, on the third day), while mice in SCP2-1 group showed lower escape latency, especially on the fourth day ($p<0.05$, compared with mod group). The swimming trajectories of the donepezil group and the SCP2-1 group were concentrated more in the target quadrant than those of the model group. However, on the fifth day, there was no significant difference in escape latency between the groups. During probe trial on the last day, the

mice with SCP2-1 treatment showed a significant increase in average time spent in the target quadrant ($p<0.05$, compared with mod group). This indicated that even though the escape latency of the model group was significantly shortened on the fifth day, the spatial memory of these animals was still inaccurate (Fig. 3H-L).

Our previous studies found that i.p. LPS could lead to weight loss in mice, in this paper, the weight changes of mice were recorded during the experiment. The results suggested that the weight of mice protected by SCP2-1 administration recovered quickly. The body weight of mice in donepezil group did not change significantly after LPS administration (Fig. 3M)

The anti-inflammatory activity of SCP1-1, a polysaccharide purified from SCP1, was shown in the supplementary Fig. 5.

[Fig. 3]

[supplementary Fig. 5]

3.2.2 Histopathology of hippocampus

H.E. staining showed that the nerve cells irregularly arranged, disordered (especially in CA1 areas), and reduced in number in the hippocampus (especially in DG areas) in the model group compared with control groups, which indicated that continuous intraperitoneal injection of LPS could induce neuroinflammation, and further lead to neuronal damage. After 3 weeks of SCP2-1 treatment, the nerve cells in the hippocampus (especially CA1) in the SCP2-1 group were arranged in good order (Fig. 4A). This suggested the neuroprotective effect of SCP2-1.

3.2.3 Activation of glial cells and proinflammatory response

GFAP is a marker for astrocytes. As shown in Fig. 4B and C, LPS stimulation increased the level of GFAP significantly ($p<0.01$, compared with Con group). Similarly, LPS remarkably enhanced the level of Iba-1 (a maker for microglia; $p<0.05$, compared with Con group) (Fig. 4 B and D). The cell body of microglia cells in LPS group was significantly larger ($p<0.05$, compared with Con group), the dendrites were

thicker, and the number of dendrites was decreased ($p<0.01$, compared with Con group), these indicated that the defense function of microglia changes. The increased levels of GFAP and Iba-1 indicate the sustained activation of glial cells. The initial activation of glial cells is beneficial to repair the pathological process of AD, but once excessively, it will induce the deposition of Aβ and aggravate AD, includes the release of pro-inflammatory cytokines. Results demonstrated that LPS significantly increased the IL-1β, IL-6 and TNF-α mRNA and protein expression levels in hippocampus. Whereas, after treatment with SCP2-1, the activation of astrocytes and microglia cells tends to normalize ($p=0.0510$ and $p<0.05$, compared with Mod group, respectively; Fig. 4 E and F). There was a prominent decrease in levels of proinflammatory cytokines after treated with SCP2-1, especially the expression of TNF-α ($p<0.05$, compared with Mod group; Fig. 4G-I).

[Fig. 4]

3.2.5 Accumulation of Aβ

Considering the important role of Aβ in AD pathology, the Aβ accumulation was investigated. Excessive deposition of Aβ induced by LPS could increase the levels of cathepsin B in the cytoplasm, induced the activation of NLRP3 and further lead to the conversion of pro-caspaes-1 to m-caspase-1. Finally, the induced increased release of pro-inflammatory factors and reduction of IL-10 and IL-4, which were the anti-inflammatory factors, disrupted the balance of glial clearance of Aβ. The results showed that there were more Aβ deposits in the hippocampus of the model group ($p<0.01$, compared with Con group), which were relieved after the administration of donepezil and SCP2-1; meanwhile, donepezil and SCP2-1 could significantly decrease the expression level of cathepsin B ($p<0.778$ and $p=0.573$, compared with Mod group) and NLRP3 ($p<0.05$ and $p<0.01$, compared with Mod group) in the hippocampus, repair transformation of caspase1 ($p<0.05$ and $p=0.064$, compared with Mod group). Donepezil and SCP2-1 also improved the level of IL-4 and IL-10, but

the effect was not obvious. This may be due to the incomplete repair of the body at the time of sample collection.

[Fig. 5]

3.2.6 NF-κB and MAPK signaling pathway in the hippocampus

As previously reported, NF-κB and MAPK signaling has been implicated in the regulation of inflammation. As shown in Fig.6, phosphorylation of IkB-α increased after stimulation of LPS compared with control group ($p<0.01$), which suggested that more NF-κB is released to participate in nuclear translocation. Accordingly, the results showed that the level of NF-κB in the nucleus increased significantly ($p<0.0001$, compared with Con group), while the level of NF-κB in the cytosolic decreased ($p<0.01$, compared with Con group). Over-activation of NF-κB is correlated with MAPK signaling pathway. As shown in Fig. 6, SCP2-1 had no effect on the ERK and JNK signaling pathways ($p>0.05$, compared with Con group), but could improve the over-phosphorylation of P38 ($p=0.0567$, compared with Con group). SB203580 (a selective inhibitor of p38MAPK) could raise the neuroprotective effect of SCP2-1($p<0.01$, compared with acute Mod group) and PMA (an activator of p38MAPK) could block the effect of SCP2-1 on neuroinflammation ($p>0.05$, compared with acute Mod group).

[Fig. 6]

4. Discussion

A growing number of studies pointed to neuroinflammation involving and playing a key role in the development of the neuropathological changes observed in AD[15, 16]. Beginning in the 1990s, several studies have shown that anti-inflammatory therapy used in diseases, such as rheumatoid arthritis, has a certain therapeutic effect on AD, demonstrating patients who are long-term anti-inflammatory drug users reducted the risk for developing AD as much as a 50%[17]. These data not only suggested the interaction between peripheral inflammation and neuroinflammation, but also demonstrated that the regulation of over-activated

inflammatory responses provides new ideas for the treatment of AD.

Some natural polysaccharides have important biological activities and functions on organism immune function[18, 19].

Due to their extensive source, accurate function and almost no side effects, immunopolysaccharides have attracted wide attention. Accordingly, many natural polysaccharides with immune activity have been shown to have the potential of anti-AD[20, 21]. In the current study, we found that SCP2-1 could improve the learning and memory impairment caused by overactive inflammation in mice, and the mechanism of SCP2-1 may be related to neuroinflammation, and we detected the changes of SCFAs in serum of mice, and found that the regulation of SCP2-1 on inflammation may be related to the improvement of gut microbiota (Supplementary Table 2 and Supplementary Fig.1)[22, 23]. Many previous studies shown that the structural characteristics of polysaccharides such as monosaccharide compositions, functional group, types of glycosidic bond, glycosidic linkage and distribution of branched units, could affected their bioactivities. Polysaccharides from *Dendrobium huoshanense*[6], *Phellinus linteus mycelia*[24] and *Sophorae tonkinensis* Radix[25] which have a →4)-α-D-Glcp-(1→ structure, and polysaccharides from *Eclipta prostrata*[26]and *Phellinus linteus* mycelia[24] which own a →4)-β-D-Galp-(1→ structure, own significant anti-inflammatory activity. The high anti-neuroinflammatory activities of SCP2-1 may be due to relatively high content of glucose and galactose and the presence of α-glycosidic bonds, which is consistent with the previous study. Additionally, a functional polysaccharides isolated from *Polygonum multiflorum*, with similar structure to SCP2-1, and has also been proved to possessed significant immunomodulatory activity, and also protecting immunocytes against 5-Fu induced immunosuppression[27].

Inflammation is closely related to Aβ. Excessive LPS could induce immune response of host to produce pro-inflammatory cytokines. IL-1β and IL-6 regulates the synthesis of APP, TNF-α can increase Aβ burden through the upregulation of β-secretase production and increased g-secretase activity[28-30]. More critically,

these inflammatory cytokines also play an important role in the clearance of Aβ. Glial cells, especially the extensively studied microglia, play an important role in neuroimmunity. While, once Aβ was phagocytosed by microglial cells, Aβ linked lysosomes adopted a swollen morphology and underwent structural damage, which lead to the loss of lysosomal integrity, and then triggers the release of lysosomal protease cathepsin B, along with the activation of NLRP3, which leaded to the conversion of procaspase-1 to maturecaspase-1[31, 32]. This process induced an increase in the release of anti-inflammatory cytokines, rather than anti-inflammatory cytokines, such as IL-4 and IL-10. This was originally a good-will act, because an increase of pro-inflammatory factors would make the body feel the threat of Aβ cause more migration of microglia to swallow Aβ[33]. In the case of AD progress, however, microglia lose the regulatory function and become more sensitive to inflammatory stimuli. Excessive inflammatory response brings malignant cycle to the body, as we mentioned earlier, a large number of pro-inflammatory cytokines will increase the deposition of Aβ, and further aggravates the pathological process of AD[34]. In this paper, we investigated the glial cells activated by LPS. As expected, astrocytes and microglia were significantly activated after LPS injection, and the deposition of Aβ was also increased significantly. The proteins related to clearance of Aβ were detected, and the results were consistent with previous studies, such as increased level of NLRP3 and more expression of mature caspase1 in the model group, while treatment of SCP2-1 can effectively alleviate these abnormalities.

Under the stimulation of immunomodulators, the IKK mediated IκB phosphorylation, and freeed the NF-κB dimer, which could continuously transfers to the nucleus and regulates transcription of genes with consistent κB binding sites in the DNA of its enhancer or promoter[35]. In this situation, the activatied NF-κB signaling pathways in microglia could consequent lead to the activation of pro-inflammatory mediators to induce exacerbate neuronal death and abnormal regulation of neuronal excitability and synaptic plasticity[36]. In addition to the NF-κB, MAPK pathways also play an improtant role in the innate immune response[8]. Previous studies have

shown that P38 is most correlated with chronic inflammation which is significantly involved in glial activation and subsequent neuroinflammation, leading to chronic neurotoxicity[37]. Therefore, we considered that the inhibitory effect of SCP2-1 on inflammatory response might be achieved by inhibiting NF-κB or MAPK pathway, and result shown that SCP2-1could decrease the nuclear translocation of NF-κB. We also examined the effect of SCP2-1 on in BV2 cells, and the results were consistent (Supplementary Fig. 2). Although SCP2-1 had no effect on ERK and JNK, it could significantly improve the phosphorylation of P38. SCP2-1 still had good anti-inflammatory effect in combination with SB203580 (PubChem CID: 176155) which had an inhibitor of P38 pathway. However, after administration of SCP2-1 combined with PMA (an activator of P38, PubChem CID: 27924), the cognition of mice and the level of pro-inflammatory cytokine in hippocampus were not significantly improved (Supplementary Fig. 4).

5. Conclusion

In this paper, we obtained a polysaccharide SCP2-1 from *S. chinensis*. The main linkages of the sugar residues were (1→4)-*α*-D-Glc and (1→4)-*β*-D-Galp. The neuroprotective effect of SCP2-1 were investigated. The results of behavioral pharmacology showed that scp2-1 could improve the memory impairment of mice caused by excessive inflammation which plays a key role in the pathological process of AD. The mechanism study showed that SCP2-1 could inhibit the sustained release of pro-inflammatory cytokines, such as TNF-α, IL-1β, regulate the level of anti-inflammatory cytokines, such as IL-4, IL-10, and balance the over activation of astrocytes and microglia, which further decrease the phagocytosis of Aβ through improve the expression of NLRP3 and M-casease-1. Therefore, the deposition of Aβ in the hippocampus of AD mice was reduced, and the pathological sections showed that the death of neurons was also reduced after SCP2-1 treatment. SCP2-1 treatment. In addition, SCP2-1 administration decreased nuclear translocation of NF-κB and over-activation of the P38 MAPK pathway to relieve the over inflammatory response. Sb203580, an inhibitor of p38, could promote the neuroprotective effect of SCP2-1.

Acknowledgements

This research was supported by the National Natural Science Foundation of China (No. 81573580). Key Laboratory of polysaccharide bioactivity evaluation of TCM of Liaoning Province. Key techniques study of consistency evaluation of drug quality and therapeutic effect (18-400-4-08) and Liaoning Distinguished Professor Project for Ying Jia (2017). Precise screening technology of Chinese traditional medicine anti-depressant active ingredients (2017LZD01). The Doctoral Scientific Research Foundation of Liaoning Province(2019-BS-233).

Conflict of interest statement

The authors declare that there are no conflicts of interest.

References

[1] J.W. Kinney, S.M. Bemiller, A.S. Murtishaw, A.M. Leisgang, A.M. Salazar, B.T. Lamb, Inflammation as a central mechanism in Alzheimer's disease, Alzheimers Dement (N Y) 4 (2018) 575-590.

[2] M. Zhu, X. Wang, L. Sun, M. Schultzberg, E. Hjorth, Can inflammation be resolved in Alzheimer's disease?, Ther Adv Neurol Disord 11 (2018) 1756286418791107.

[3] S.A. Wolf, H.W. Boddeke, H. Kettenmann, Microglia in Physiology and Disease, Annu Rev Physiol 79 (2017) 619-643.

[4] L. Zhong, Y. Xu, R. Zhuo, T. Wang, K. Wang, R. Huang, D. Wang, Y. Gao, Y. Zhu, X. Sheng, K. Chen, N. Wang, L. Zhu, D. Can, Y. Marten, M. Shinohara, C.C. Liu, D. Du, H. Sun, L. Wen, H. Xu, G. Bu, X.F. Chen, Soluble TREM2 ameliorates pathological phenotypes by modulating microglial functions in an Alzheimer's disease model, Nat Commun 10(1) (2019) 1365.

[5] T. Wisniewski, F. Goni, Immunotherapeutic approaches for Alzheimer's disease, Neuron 85(6) (2015) 1162-76.

[6] J.C. Ge, X.Q. Zha, C.Y. Nie, N.J. Yu, Q.M. Li, D.Y. Peng, J. Duan, L.H. Pan, J.P. Luo, Polysaccharides from Dendrobium huoshanense stems alleviates lung inflammation in cigarette smoke-induced mice, Carbohydr Polym 189 (2018) 289-295.

[7] X. Chen, R. Tang, T. Liu, W. Dai, Q. Liu, G. Gong, S. Song, M. Hu, L. Huang, Z. Wang, Physicochemical properties, antioxidant activity and immunological effects in vitro of polysaccharides from Schisandra sphenanthera and Schisandra chinensis, Int J Biol Macromol 131 (2019) 744-751.

[8] X. Cao, D. Liu, Y. Xia, T. Cai, Y. He, J. Liu, A novel polysaccharide from Lentinus edodes mycelia protects MIN6 cells against high glucose-induced damage via the MAPKs and Nrf2 pathways, Food Nutr Res 63 (2019).

[9] M.G. Dilshara, R.G. Jayasooriya, C.H. Kang, S. Lee, S.R. Park, J.W. Jeong, Y.H. Choi, Y.T. Seo, Y.P. Jang, G.Y. Kim, Downregulation of pro-inflammatory mediators by a water extract of Schisandra chinensis (Turcz.) Baill fruit in lipopolysaccharide-stimulated RAW 264.7 macrophage cells, Environ Toxicol Pharmacol 36(2) (2013) 256-64.

[10] Y. Takimoto, H.Y. Qian, E. Yoshigai, T. Okumura, Y. Ikeya, M. Nishizawa, Gomisin N in the herbal drug gomishi (Schisandra chinensis) suppresses inducible nitric oxide synthase gene via C/EBPbeta and NF-kappaB in rat hepatocytes, Nitric Oxide 28 (2013) 47-56.

[11] T. Zhao, G. Mao, M. Zhang, W. Feng, R. Mao, Y. Zhu, X. Gu, Q. Li, L. Yang, X. Wu, Structure analysis of a bioactive heteropolysaccharide from Schisandra chinensis (Turcz.) Baill, Carbohydr Polym 103 (2014) 488-95.

[12] M. Xu, T. Yan, K. Fan, M. Wang, Y. Qi, F. Xiao, K. Bi, Y. Jia, Polysaccharide of Schisandra Chinensis Fructus ameliorates cognitive decline in a mouse model of Alzheimer's disease, J Ethnopharmacol 237 (2019) 354-365.

[13] Y. Rong, R. Yang, Y. Yang, Y. Wen, S. Liu, C. Li, Z. Hu, X. Cheng, W. Li, Structural characterization of an active polysaccharide of longan and evaluation of immunological activity, Carbohydr Polym 213 (2019) 247-256.

[14] Y. Wang, N. Zhang, J. Kan, X. Zhang, X. Wu, R. Sun, S. Tang, J. Liu, C. Qian, C. Jin, Structural characterization of water-soluble polysaccharide from Arctium lappa and its effects on colitis mice, Carbohydr Polym 213 (2019) 89-99.

[15] L. Tiozzo Fasiolo, M.D. Manniello, F. Bortolotti, F. Buttini, A. Rossi, F. Sonvico, P. Colombo, G. Valsami, G. Colombo, P. Russo, Anti-inflammatory flurbiprofen nasal powders for nose-to-brain delivery in Alzheimer's disease, J Drug Target 27(9) (2019) 984-994.

[16] L. Chen, L. Hu, J. Zhao, H. Hong, F. Feng, W. Qu, W. Liu, Chotosan improves Abeta1-42-induced cognitive impairment and neuroinflammatory and apoptotic responses through the inhibition of TLR-4/NF-kappaB signaling in mice, J Ethnopharmacol 191 (2016) 398-407.

[17] A. Dhingra., B. Chopra., Inflammation as a Therapeutic Target for Various Deadly Disorders: A Review, Curr Drug Targets 43(4) (2019) 817-29.

[18] X. Luo, S. Huang, S. Luo, H. Liao, Y. Wang, X. Deng, F. Ma, C.W. Ma, L. Zhou, Identification of genes underlying the enhancement of immunity by a formula of lentinan, pachymaran and tremelia polysaccharides in immunosuppressive mice, Sci Rep 8(1) (2018) 10082.

[19] Y.R. Seo, D.K. Patel, W.C. Shin, W.S. Sim, O.H. Lee, K.T. Lim, Structural Elucidation and Immune-Enhancing Effects of Novel Polysaccharide from Grifola frondosa, Biomed Res Int 2019 (2019) 7528609.

[20] W. Chen, X. Cheng, J. Chen, X. Yi, D. Nie, X. Sun, J. Qin, M. Tian, G. Jin, X. Zhang, Lycium barbarum polysaccharides prevent memory and neurogenesis impairments in scopolamine-treated rats,

PLoS One 9(2) (2014) e88076.

[21] Y.-C. Huang, H.-J. Tsay, M.-K. Lu, C.-H. Lin, C.-W. Yeh, H.-K. Liu, Y.-J. Shiao, Astragalus membranaceus-Polysaccharides Ameliorates Obesity, Hepatic Steatosis, Neuroinflammation and Cognition Impairment without Affecting Amyloid Deposition in Metabolically Stressed APPswe/PS1dE9 Mice, International Journal of Molecular Sciences 18(12) (2017).

[22] R. Russo, C. Cristiano, C. Avagliano, C. De Caro, G. La Rana, G.M. Raso, R.B. Canani, R. Meli, A. Calignano, Gut-brain Axis: Role of Lipids in the Regulation of Inflammation, Pain and CNS Diseases, Curr Med Chem 25(32) (2018) 3930-3952.

[23] L. Zhang, Y. Wang, X. Xiayu, C. Shi, W. Chen, N. Song, X. Fu, R. Zhou, Y.F. Xu, L. Huang, H. Zhu, Y. Han, C. Qin, Altered Gut Microbiota in a Mouse Model of Alzheimer's Disease, J Alzheimers Dis 60(4) (2017) 1241-1257.

[24] T. Hu, Q. Lin, T. Guo, T. Yang, W. Zhou, X. Deng, J.K. Yan, Y. Luo, M. Ju, F. Luo, Polysaccharide isolated from Phellinus linteus mycelia exerts anti-inflammatory effects via MAPK and PPAR signaling pathways, Carbohydr Polym 200 (2018) 487-497.

[25] L. Cai, S. Zou, D. Liang, L. Luan, Structural characterization, antioxidant and hepatoprotective activities of polysaccharides from Sophorae tonkinensis Radix, Carbohydr Polym 184 (2018) 354-365.

[26] N. Li, S. Shi, F. Yang, H. Wang, J. Su, F. Huang, H. Wu, X. Wu, S. Wang, A polysaccharide from Eclipta prostrata alleviates experimental autoimmune encephalomyelitis through inhibiting Th17 cells, Carbohydr Polym 201 (2018) 608-614.

[27] Q. Zhang, Y. Xu, J. Lv, M. Cheng, Y. Wu, K. Cao, X. Zhang, X. Mou, Q. Fan, Structure characterization of two functional polysaccharides from Polygonum multiflorum and its immunomodulatory, Int J Biol Macromol 113 (2018) 195-204.

[28] K. Schmidt, M. Wienken, C.W. Keller, P. Balcarek, C. Munz, J. Schmidt, IL-1beta-Induced Accumulation of Amyloid: Macroautophagy in Skeletal Muscle Depends on ERK, Mediators Inflamm 2017 (2017) 5470831.

[29] F. Kramer, J. Torzewski, J. Kamenz, K. Veit, V. Hombach, J. Dedio, Y. Ivashchenko, Interleukin-1beta stimulates acute phase response and C-reactive protein synthesis by inducing an NFkappaB- and C/EBPbeta-dependent autocrine interleukin-6 loop, Mol Immunol 45(9) (2008) 2678-89.

[30] E. Paouri, O. Tzara, S. Zenelak, S. Georgopoulos, Genetic Deletion of Tumor Necrosis Factor-alpha Attenuates Amyloid-beta Production and Decreases Amyloid Plaque Formation and Glial Response in the 5XFAD Model of Alzheimer's Disease, J Alzheimers Dis 60(1) (2017) 165-181.

[31] Y. Hong, Y. Liu, D. Yu, M. Wang, Y. Hou, The neuroprotection of progesterone against Abeta-induced NLRP3-Caspase-1 inflammasome activation via enhancing autophagy in astrocytes, Int Immunopharmacol 74 (2019) 105669.

[32] A. Luciunaite, R.M. McManus, M. Jankunec, I. Racz, C. Dansokho, I. Dalgediene, S. Schwartz, F. Brosseron, M.T. Heneka, Soluble Abeta Oligomers and Protofibrils Induce NLRP3 Inflammasome Activation in Microglia, J Neurochem (2019) e14945.

[33] A. Lyons, R.J. Griffin, C.E. Costelloe, R.M. Clarke, M.A. Lynch, IL-4 attenuates the neuroinflammation induced by amyloid-beta in vivo and in vitro, J Neurochem 101(3) (2007) 771-81.

[34] A. Katsumoto, H. Takeuchi, K. Takahashi, F. Tanaka, Microglia in Alzheimer's Disease: Risk Factors and Inflammation, Front Neurol 9 (2018) 978.

[35] E.C. Dresselhaus, M.K. Meffert, Cellular Specificity of NF-kappaB Function in the Nervous System, Front Immunol 10 (2019) 1043.

[36] H. Lee, D.S. Lee, K.J. Chang, S.H. Kim, S.H. Cheong, Glucose-Taurine Reduced Exerts Neuroinflammatory Responses by Inhibition of NF-kappaB Activation in LPS-Induced BV2 Microglia, Adv Exp Med Biol 1155 (2019) 857-867.

[37] I. Patraca, N. Martinez, O. Busquets, A. Marti, I. Pedros, C. Beas-Zarate, M. Marin, M. Ettcheto, F. Sureda, C. Auladell, A. Camins, J. Folch, Anti-inflammatory role of Leptin in glial cells through p38 MAPK pathway inhibition, Pharmacol Rep 69(3) (2017) 409-418.

Table Captions

Table 1. Methylation analysis for SCP2-1

Table 2. Chemical shifts of C and H atom (ppm)

Table 1. Methylation analysis for SCP2-1

RT	Methylated sugar	Mass fragments (m/z)	Molar ratios	Linkage type
18.794	2,3,4,6-Me_4-Galp	43,71,87,101,117,129,145,161,205	3.25	1-linked-Galp
23.774	2,3,6-Me_3-Galp	43,87,99,101,113,117,129,131,161,173,233	10.88	1, 4-linked-Galp
24.086	2,3,6-Me_3-Glcp	43,87,99,101,113,117,129,131,161,173,233	82.62	1, 4- linked-Glcp
30.343	2,3-Me_2-Galp	43,71,85,87,99,101,117,127,159,161,201	3.25	1,4,6-linked-Galp

Table 2. ^{1}H and ^{13}C NMR spectroscopic data (ppm)

Glycosyl residues	H1 C1	H2 C2	H3 C3	H4 C4	H5 C5	H6a C6	H6b
1,4-*α*-Glcp (A)	5.32	3.55	3.89	3.57	3.76	3.78	3.75
	101.0	72.9	74.6	78.2	72.5	61.8	
1,4-*β*-Galp (B)	4.57	3.61	3.70	4.10	3.64	3.72	ns
	105.7	73.1	74.3	79.0	75.9	62.1	
1,4,6-*β*-Galp (C)	4.40	3.22	3.48	3.87	4.03	3.70	3.81
	103.0	74.7	74.7	78.2	69.9	69.9	
1-*β*-Galp (D)	4.56	3.36	3.88	3.86	3.71	3.72	ns
	105.8	70.7	72.9	69.9	74.7	62.1	

Figure Captions

Fig. 1. The separation flow diagram of SCP2-1

Fig. 2. Monosaccharide composition and NMR spectra of SCP2-1. A. Monosaccharide composition B. ^{1}H-NMR. C. ^{13}C and Dept135 NMR. D. ^{1}H-^{1}H COSY. E. NOESY. F. HSQC. G. HMBC. H. The possible structure of SCP2-1.

Fig. 3. The influence of SCP2-1 on learning and memory in mice (n=10-12). A. The experimental schedule of animal experiment. B-D. Diagram, the percent of novel arm entries to total arm entries (%) and number of arm entries in Y maze test. E-G. Diagram, the exploration time of novel object and familiar object and the exploration index of mice in NOR tests. H-L. Diagram, the escape latency of mice and the swimming path of mice in place navigation test, and the percentage of time that mice in the target quadrant in the spatial probe test. M. The changes in the weight during LPS injection, and the range of weight varies from 4g to-4g. Four mice in each group were randomly selected to record their weight changes. As shown on the right, the more weight the mice lose, the greener they are, and the more weight they gain, the redder they are. *$p<0.05$, **$p<0.01$ c and ***$p<0.001$compared with model group.

Fig. 4. The influence of SCP2-1 on hippocampus of mice. A. histopathology with HE staining. B. The activation of astrocyte and microglia. Stained hippocampus with antibodies against GFAP or Iba-1 (red). Nuclei were stained with DAPI (blue). C and D. IOD of GFAP and Iba-1. G. The protein levels and mRNA levels of TNF-α released. H. The protein levels and mRNA levels of IL-1β released. I. The protein levels and mRNA levels of IL-6 released. The arrow points to nuclear retraction or the activated GFAP and Iba-1. Magnification: 200x.

Fig. 5. The influence of SCP2-1 on accumulation of Aβ. A. Representative photographs for CA1. Magnification: 200×. B. Representative band of cathepsin B in cytosolic, NLRP3, M-caspase-1, Pro-caspase-1, IL-4, IL-10 and their control protein β-actin. C. IOD of the $A\beta_{1-42}$. D-H. Relative level of cathepsin B, NLRP3 to β-actin, M-caspeaes-1 to pro-caspase-1, IL-4 and IL-10 to β-actin. Results are represented as mean ± SEM (n = 3). *p<0.05, **p<0.01 and ***p<0.001 compared with model group. The arrow points to accumulation of Aβ.

Fig. 6. Effects of SCP2-1 on the NF-κB and MAPK signaling pathway in the hippocampus. A. Representative bands and levels of NF-κB in nuclear and cytosolic. B. Representative bands and levels of p-IκB-α to IκB-α. C and D. Representative bands and levels of iNOS and COX2 to β-actin. E-G. Representative bands and levels of p-ERK to ERK, p-JNK to JNK and p-P38 to P38. Results are represented as mean ± SEM (n = 3). *p<0.05, **p<0.01 and ***p<0.001 compared with control group.

INTERNATIONAL JOURNAL OF BIOLOGICAL MACROMOLECULES

MengjieXu[a#], Tingxu Yan[b#], Guowei Gong[c], Bo Wu[b], Bosai He[b], Yiyang Du[b], Feng Xiao[b*], Ying Jia[b*]

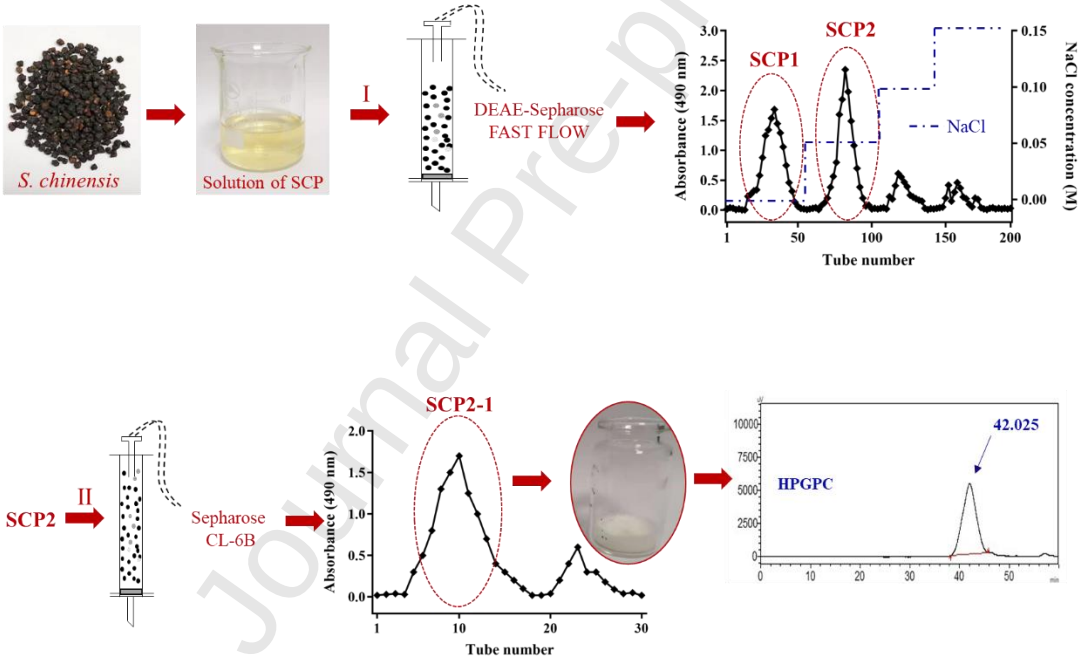

Fig. 1. The separation flow diagram of SCP2-1

INTERNATIONAL JOURNAL OF BIOLOGICAL MACROMOLECULES

MengjieXu[a#], Tingxu Yan[b#], Guowei Gong[c], Bo Wu[b], Bosai He[b], Yiyang Du[b], Feng Xiao[b*], Ying Jia[b*]

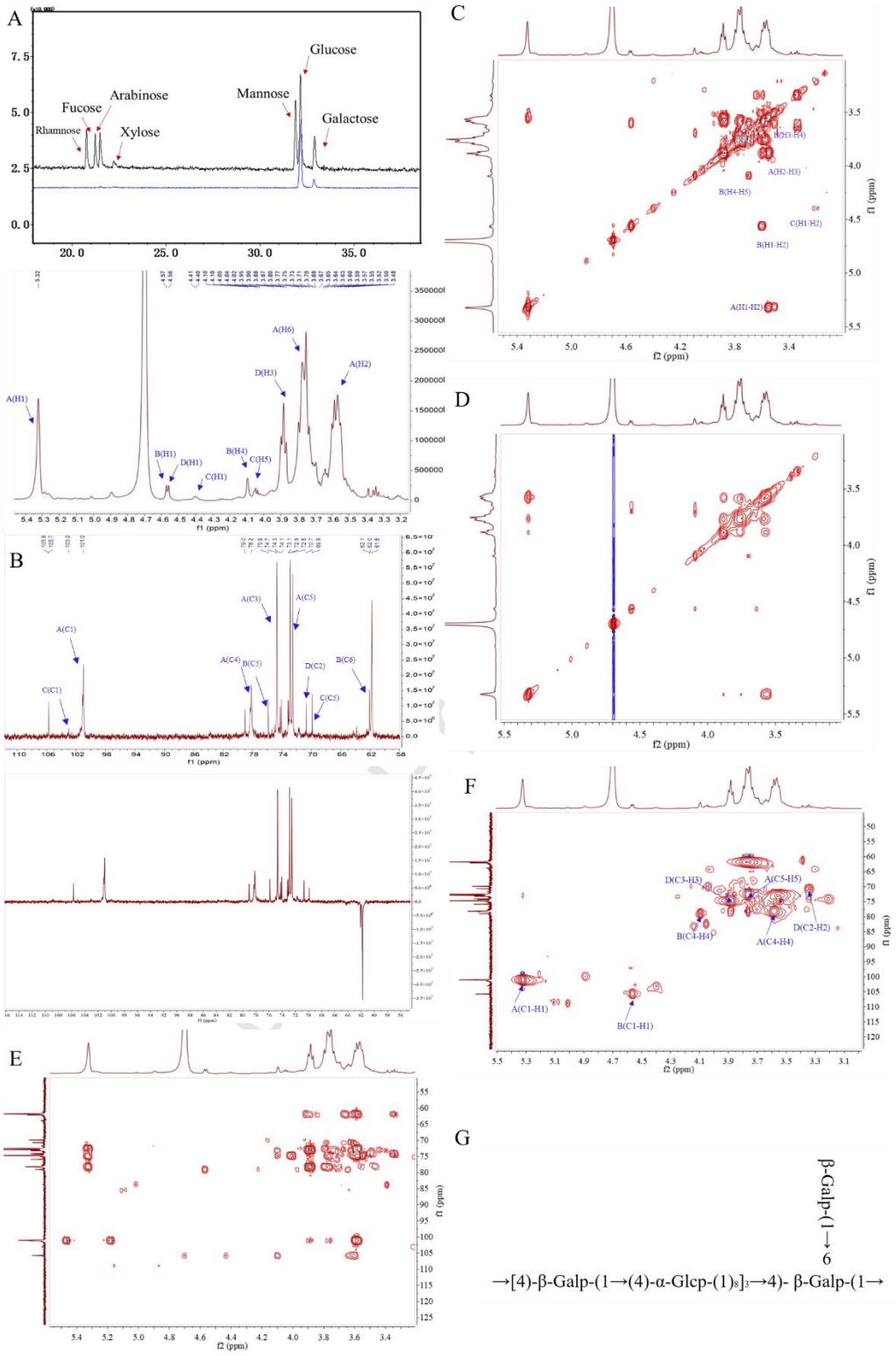

Fig. 2. Monosaccharide composition and NMR spectra of SCP2-1. A. Monosaccharide composition B. ^{1}H-NMR. C. ^{13}C and Dept135 NMR. D. ^{1}H-^{1}H COSY. E. NOESY. F. HSQC. G. HMBC. H. The possible structure of SCP2-1.

MengjieXu[a#], Tingxu Yan[b#], Guowei Gong[c], Bo Wu[b], Bosai He[b], Yiyang Du[b], Feng Xiao[b*], Ying Jia[b*]

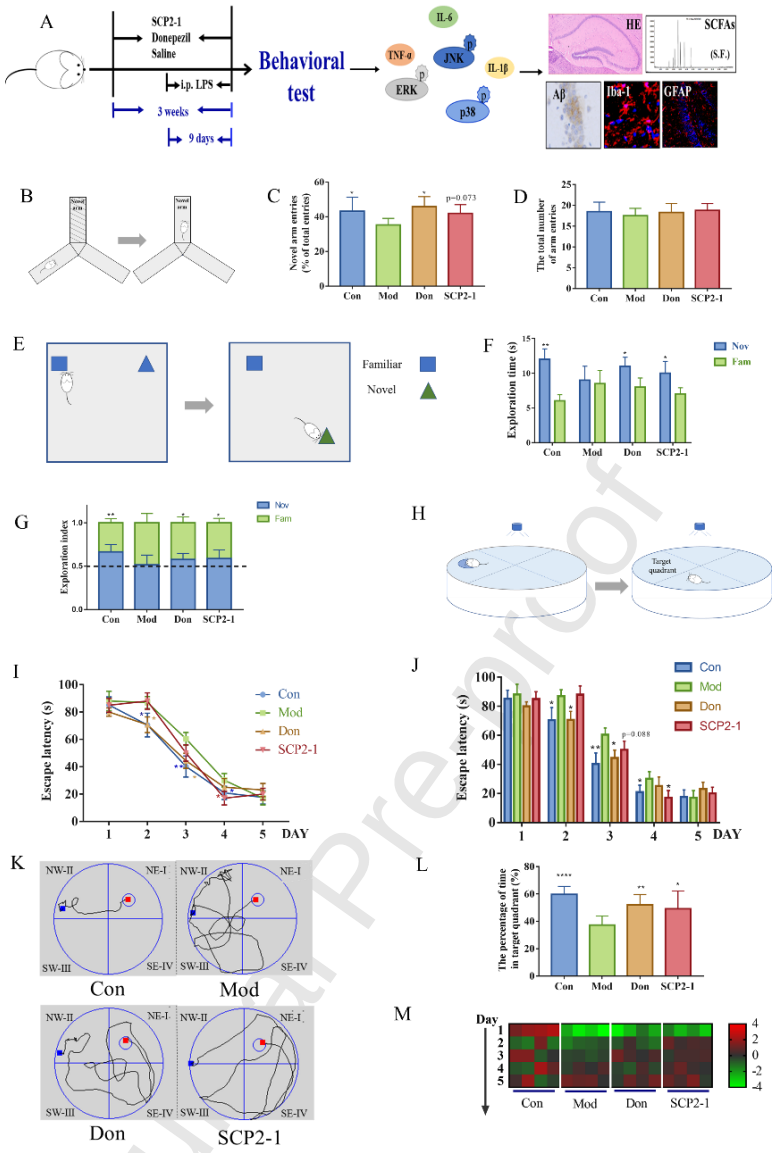

Fig. 3. The influence of SCP2-1 on learning and memory in mice (n=10-12). A. The experimental schedule of animal experiment. B-D. Diagram, the percent of novel arm entries to total arm entries (%) and number of arm entries in Y maze test. E-G. Diagram, the exploration time of novel object and familiar object and the exploration index of mice in NOR tests. H-L. Diagram, the escape latency of mice and the swimming path of mice in place navigation test, and the percentage of time that mice in the target quadrant in the spatial probe test. M. The changes in the weight during LPS injection, and the range of weight varies from 4g to-4g. Four mice in each group were randomly selected to record their weight changes. As shown on the right, the more weight the mice lose, the greener they are, and the more weight they gain, the redder they are. *p<0.05, **p<0.01 c and ***p<0.001compared with model group.

INTERNATIONAL JOURNAL OF BIOLOGICAL MACROMOLECULES

MengjieXu[a#], Tingxu Yan[b#], Guowei Gong[c], Bo Wu[b], Bosai He[b], Yiyang Du[b], Feng Xiao[b*], Ying Jia[b*]

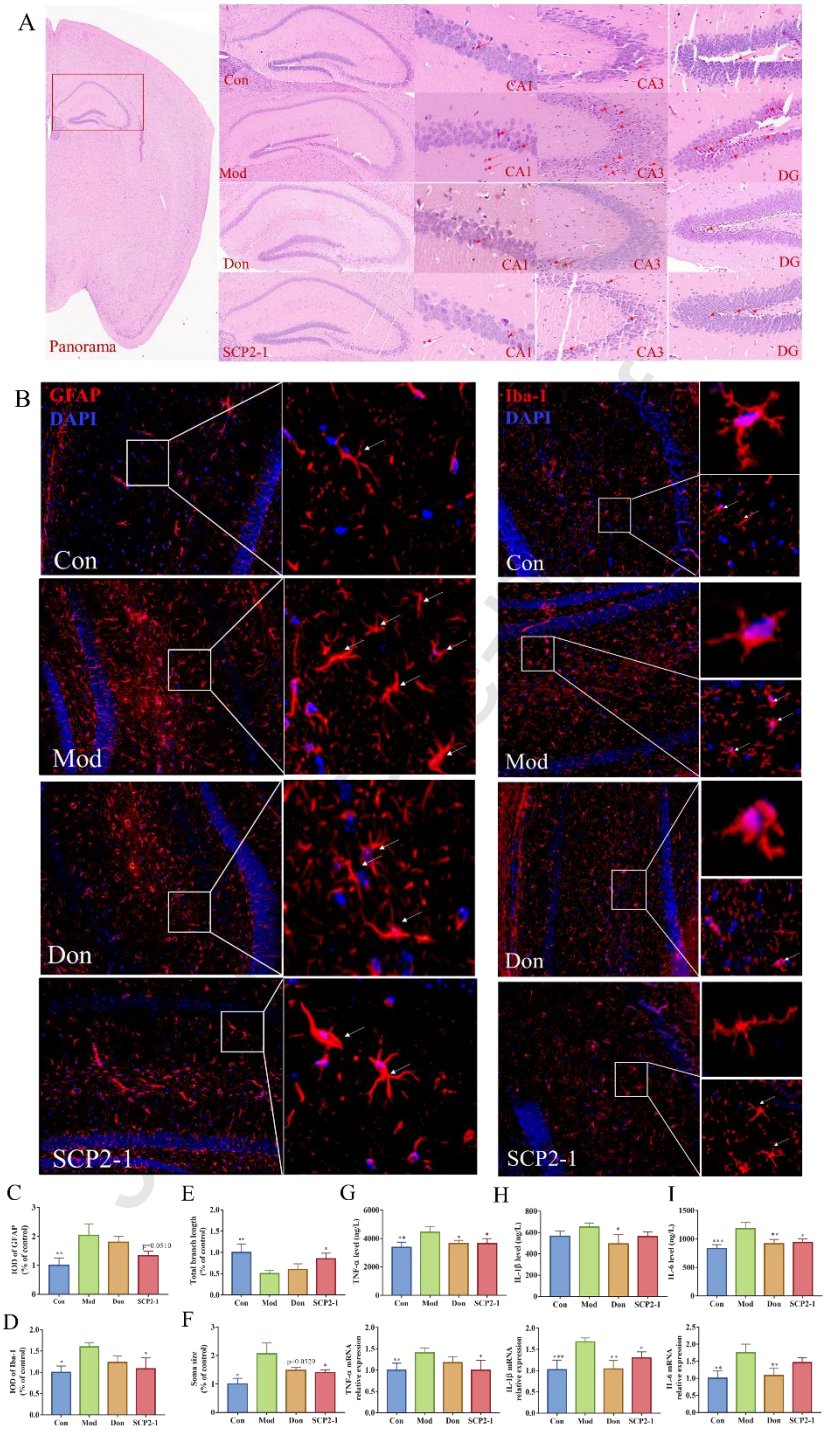

Fig. 4. The influence of SCP2-1 on hippocampus of mice. A. histopathology with HE staining. B. The activation of astrocyte and microglia. Stained hippocampus with antibodies against GFAP or Iba-1 (red). Nuclei were stained with DAPI (blue). C and D. IOD of GFAP and Iba-1. G. The protein levels and mRNA levels of TNF-α released. H.

The protein levels and mRNA levels of IL-1β released. I. The protein levels and mRNA levels of IL-6 released. The arrow points to nuclear retraction or the activated GFAP and Iba-1. Magnification: 200×.

INTERNATIONAL JOURNAL OF BIOLOGICAL MACROMOLECULES

MengjieXu[a#], Tingxu Yan[b#], Guowei Gong[c], Bo Wu[b], Bosai He[b], Yiyang Du[b], Feng Xiao[b*], Ying Jia[b*]

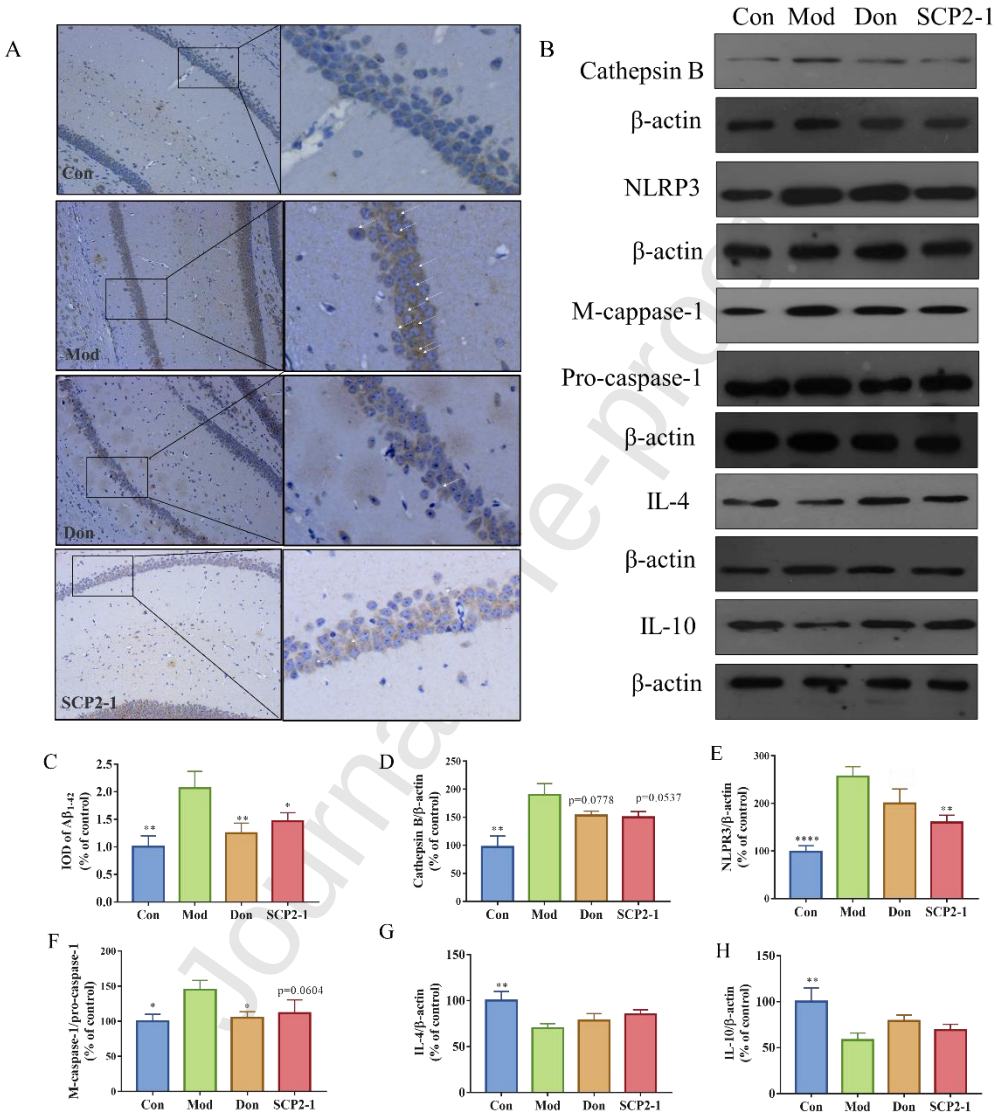

Fig. 5. The influence of SCP2-1 on accumulation of Aβ. A. Representative photographs for CA1. Magnification: 200x. B. Representative band of cathepsin B in cytosolic, NLRP3, M-caspase-1, Pro-caspase-1, IL-4, IL-10 and their control protein β-actin. C. IOD of the $Aβ_{1-42}$. D-H. Relative level of cathepsin B, NLRP3 to β-actin, M-caspeaes-1 to pro-caspase-1, IL-4 and IL-10 to β-actin. Results are represented as mean ± SEM (n = 3). *p<0.05, **p<0.01 and ***p<0.001 compared with model group. The arrow points to accumulation of Aβ.

INTERNATIONAL JOURNAL OF BIOLOGICAL MACROMOLECULES

MengjieXu[a#], Tingxu Yan[b#], Guowei Gong[c], Bo Wu[b], Bosai He[b], Yiyang Du[b], Feng Xiao[b*], Ying Jia[b*]

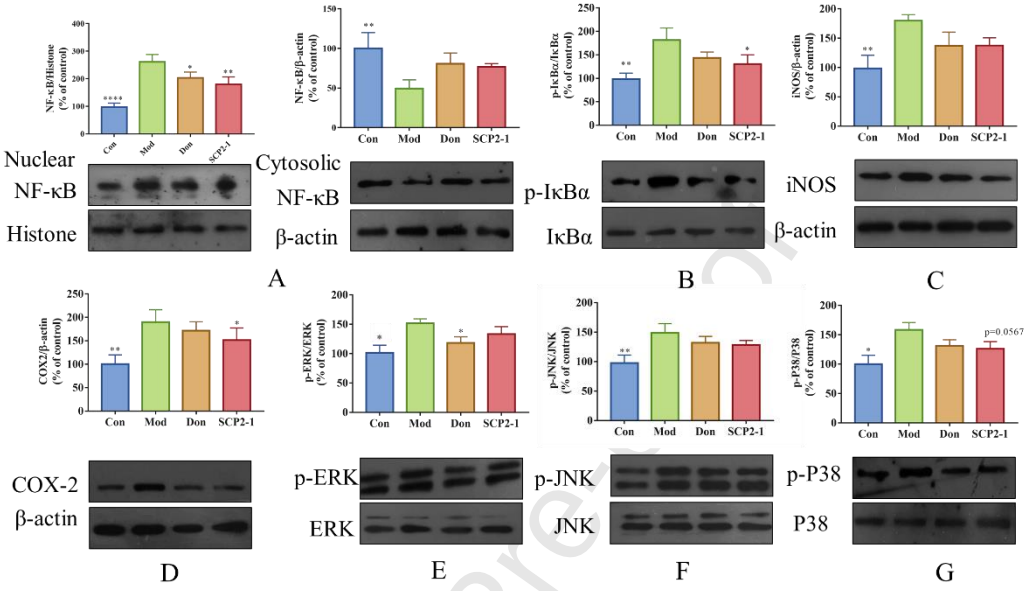

Fig. 6. Effects of SCP2-1 on the NF-κB and MAPK signaling pathway in the hippocampus. A. Representative bands and levels of NF-κB in nuclear and cytosolic. B. Representative bands and levels of p-IκB-α to IκB-α. C and D. Representative bands and levels of iNOS and COX2 to β-actin. E-G. Representative bands and levels of p-ERK to ERK, p-JNK to JNK and p-P38 to P38. Results are represented as mean ± SEM (n = 3). *p<0.05, **p<0.01 and ***p<0.001 compared with control group.

MengjieXu: Conceptualization, Methodology, Investigation, Writing - Original Draft. **Tingxu Yan:** Conceptualization, Formal analysis, Writing - Review & Editing, Project administration. **Guowei Gong**：Writing - Review & Editing. **Bo Wu**: Resources, Writing - Review & Editing. **Bosai He:** Writing - Review & Editing. **Yiyang Du** Writing - Review & Editing. **Feng Xiao:** Writing - Review & Editing, Resources. **Ying Jia**: Resources, Writing - Review & Editing, Supervision, Funding acquisition.